Cancer Letters 443 (2019) 135–144

Contents lists available at ScienceDirect

Cancer Letters

journal homepage: www.elsevier.com/locate/canlet

Original Articles

Phosphatidyl inositol 3-kinase (PI3K)-mTOR inhibitor PKI-402 inhibits breast cancer induced osteolysis

Guixin Yuan[a,1], Zhen Lian[a,1], Qian Liu[b,c], Xixi Lin[b,c], Dantao Xie[a], Fangming Song[b,c], Xinjia Wang[a], Siyuan Shao[b,c], Bo Zhou[c,d,e], Chen Li[b,c], Muyan Li[d,**], Guanfeng Yao[a,*]

[a] Department of Orthopedics, The Second Affiliated Hospital, Shantou University Medical College, Shantou, Guangdong, 515041, China
[b] Research Centre for Regenerative Medicine, The First Affiliated Hospital of Guangxi Medical University, Guangxi Medical University, Guangxi, 530021, China
[c] Guangxi Key Laboratory of Regenerative Medicine, Guangxi Medical University, Guangxi, 530021, China
[d] Guangxi Collaborative Innovation Center for Biomedicine, Guangxi Medical University, Nanning, Guangxi, 530021, China
[e] Orthopaedic Department, The First Affiliated Hospital of Guangxi Medical University, Guangxi Medical University, Guangxi, 530021, China

ARTICLE INFO

Keywords:
Bone metastasis
PI3K-mTOR-AKT-Signaling pathway
MDA-MB-231 cells
Osteoclast
Bone destruction

ABSTRACT

Bone metastasis causes bone pain and pathological bone fracture in breast cancer patients with a serious complication. Previous studies have demonstrated that a novel phosphatidyl inositol 3-kinase (PI3K)-mTOR inhibitor PKI-402 suppressed the growth of breast cancer cells. However, the role of PKI-402 involved in osteolysis induced by breast cancer remains unclear. In this study, we showed that treatment of PKI-402 led to significant decreases in RANKL-induced osteoclastogenesis and osteoclast-specific gene expression in mouse bone marrow-derived macrophages and reduced proliferation, migration and invasion of MDA-MB-231 breast cancer cells by blocking the PI3K-AKT-mTOR signaling pathway. Importantly, as evidenced by the observation that the administration of PKI-402 inhibited MDA-MB-231-induced osteolysis *in vivo*, PKI-402 exerted an inhibitory effect on osteoclast formation and bone resorption, critical for cancer cells-induced bone destruction. These results strongly suggest that PKI-402 might have a therapeutic potential to inhibit breast cancer induced osteolysis.

1. Introduction

Breast cancer is the most common cancer among Chinese women, and it accounts for approximately 12.2% of all new cancer patients in China, and 9.6% of all cancer deaths worldwide [1]. Approximately 75–80% of patients with advanced-stage breast cancer develop distant bone metastasis [2], which results in osteolysis that lead to symptoms of bone pain, pathological fractures, hypercalcaemia and spinal cord compression [3]. Currently, there are no effective therapeutic treatment options available for bone metastasis mediated by breast cancer. Thus, investigating potential compounds that block the signaling pathways involved in the osteolysis process of breast cancer cells, especially for the colonization of cancer cells into bones is of great importance.

Phosphoinositide 3-kinase (PI3K)-AKT-mTOR pathway is one of the most common signaling pathways involved in tumorigenesis of various cancer types [4,5]. It plays critical roles in regulating cell proliferation, apoptosis, invasion and metastasis of cancer [6]. Several inhibitors of the PI3K-AKT-mTOR pathway have been in the stage of the preclinical development as well as clinical trials [7–9]. One of them is PKI-402 which previously exhibited suppression of cell proliferation of breast cancer MDA-MB-361 and MDA-MB-468 cell lines, colon cancer HCT116 and HT29 cell lines, and lung cancer NCI−H157 cell line *in vitro*, and tumor growth in xenograft models [10,11].

Although PKI-402 has been shown to suppress the formation of local tumors, the role of this compound involved in breast cancer-induced osteolysis remains unclear. Therefore, the current study investigated its effect on breast cancer induced osteolysis *in vitro* and *in vivo*. The results showed that PKI-402 suppressed the growth, migration and invasion of breast cancer cells, osteoclast formation and bone resorption. Furthermore, using the mouse model of breast cancer-induced osteolysis that breast cancer cells were injected into tibias, we found the administration of this inhibitor led to a significant decrease in tumor volume in bones and the reversal of bone disruption. Our data strongly suggested that PKI-402 is a potential therapeutic molecule for the treatment of osteolysis caused by breast cancer.

* Corresponding author.
** Corresponding author.
E-mail addresses: dxbutterfly@163.com (M. Li), yao_guanfeng@hotmail.com (G. Yao).
[1] Guixin Yuan and Zhen Lian contributed equally to this work.

https://doi.org/10.1016/j.canlet.2018.11.038
Received 28 July 2018; Received in revised form 26 November 2018; Accepted 29 November 2018

2. Materials and methods

2.1. Materials

PKI-402 was purchased from Selleck Chemicals (Houston, TX, USA). It was dissolved in dimethyl sulfoxide (DMSO) at a stock concentration of 20 mM and stored at −20 °C. It was freshly diluted to the desired concentration with complete culture medium so that the final concentration of DMSO was no more than 0.05% (v/v). The animal experimental procedures and animal facility were approved by the Animal Care and Welfare Committee of Guangxi Medical University (SYXK2009-0004). Dulbecco's Modified Eagle's Medium (DMEM), Alpha-Modified Minimum Essential Medium (α-MEM) and Fetal Bovine Serum (FBS) were obtained from Gibco BRL (Gaithersburg, MD, USA). The MTS-based cell proliferation assay kit was purchased from Promega (Madison, WI, USA). Mouse macrophage colony-stimulating factor (M-CSF) and recombinant GST-rRANKL were purchased from R&D Systems (Minneapolis, MN, USA). Primary antibodies against p-PI3K p85/p55, PI3K p85, AKT, p-AKT (Thr308), p-mTOR (Ser2448), mTOR and β-actin, and secondary antibodies were obtained from Cell Signaling Technology (Danvers, MA, USA). Anti-Cathepsin K and Anti-Caspase-3 antibodies were obtained from Abcam (MA, USA). The tartrate-resistant acid phosphatase (TRAP) staining kit, Triton X-100 and all other reagents were purchased from Sigma-Aldrich (St. Louis, MO, USA), unless otherwise noted.

2.2. MTS cell proliferation assay

The effect of PKI-402 on proliferation of BMMs and MDA-MB-231 cells was evaluated by the MTS assay. MDA-MB-231 cells were obtained from the American Type Culture Collection (Manassas, VA, USA) and cultured in DMEM containing L-glutamine, phenol red, L-cysteine, L-methionine and sodium bicarbonate and supplemented with 10% FBS and 1% penicillin/streptomycin. Long bone BMMs were seeded into a 96-well plate at a density of 6×10^3 cells/well in complete α-MEM with 30 ng/mL M-CSF for 24 h and then incubated with the indicated concentrations of PKI-402 (0–2.5 μM) for 24, 48, 72 and 96 h respectively. Subsequently 20 μl MTS buffer was added to cells in each well and incubated for 2 h at 37 °C. The absorbance at the wavelength of 490 nm was measured on the ELx800 TM enzyme scale (Bio-Tek Instruments, Winooski, VT, USA). The half maximal inhibitory concentration (IC_{50}) of PKI-402 were calculated by GraphPad Prism v.7.0c software (San Diego, CA, USA).

2.3. Osteoclastogenesis assay

For *in vitro* osteoclastogenesis assay, bone marrow-derived macrophages (BMMs) were extracted from C57BL/6 mice and cultured in α-MEM supplemented with 10% FBS, 100 U/mL penicillin, 100 mg/mL streptomycin and 30 ng/ml M-CSF. Cells were incubated at 37 °C in a humidified incubator maintained in a 5% CO_2 atmosphere. After 3 days, cells were seeded into a 96-well plate at a density of 6×10^3 cells/well in triplicate with 30 ng/ml M-CSF and 50 ng/ml RANKL in the absence or presence of PKI-402 (0, 0.02, 0.04, 0.08 μM). The medium was refreshed every two days until the formation of multinucleated osteoclasts. The cells were washed with PBS twice, fixed by 4% paraformaldehyde for 20 min, and stained with tartrate-resistant acid. TRAP-positive cells, which exhibited more than three nuclei were identified as osteoclasts and the number of which was calculated under a microscope (Leica, Germany).

2.4. Hydroxyapatite resorption assay

Bone resorption assay was carried out using a hydroxyapatite 96-well plate (Corning, NY, USA) according to the manufacturer's instructions. BMMs seeded onto 6-well plates were stimulated with 50 ng/mL RANKL and 30 ng/mL M-CSF until the formation of pre-mature osteoclasts. Cells were gently digested and re-seeded onto a hydroxyapatite 96-well plate with various concentrations of PKI-402 (0, 0.02, 0.04 or 0.08 μM) in triplicate. After 48 h, half of the wells fixed by 4% paraformaldehyde for 20 min, and stained with tartrate-resistant acid phosphatase. TRAP-positive cells, which exhibited more than three nuclei were identified as osteoclasts and the number of osteoclasts was calculated under a microscope (Leica, Germany). The other half of the wells were washed with 5% sodium hypochlorite for 5 min and the resorption were photographed under a standard light microscope (Leica, Germany). The percentage of hydroxyapatite surface area resorbed by the osteoclasts was quantified by ImageJ software (NIH, Bethesda, MD).

2.5. Immunofluorescent staining

BMMs were seeded into a 96-well plate at a density of 6×10^3 cells/well in triplicate with 30 ng/ml M-CSF and 50 ng/ml RANKL in the absence or presence of PKI-402 (0, 0.02, 0.04, 0.08 μM). The medium was refreshed every two days until the formation of multinucleated osteoclasts. The cells were washed with PBS twice and fixed by 4% paraformaldehyde for 20 min. After permeabilized with 0.1% Triton X-100 PBS and blocked with 3% BSA in PBS, cells were stained by Rhodamine-conjugated phalloidin for 1 h in dark and the nuclei were counterstained with DAPI and mounted and photographed by fluorescence microscope (Leica, Germany).

2.6. Transwell invasion assay

The Transwell invasion assay was performed on a 24-well plate equipped with an 8 μm pore polycarbonate filter on each well. MDA-MB-231 cells were seeded at a density of 5×10^4 cells/well into Transwell inserts in 200 μl of serum-free media with the indicated concentrations of PKI-402 (0, 0.02, 0.04, and 0.08 μM) in triplicate. The lower chambers were filled with 600 μl complete media and cells were incubated at 37 °C for 24 h. After cells on the top of Transwell inserts that did not pass through the filter were removed by cotton-tipped applicators, cells in the lower chambers were fixed by 4% paraformaldehyde for 30 min, and stained with 0.2% crystal violet. Then cells were imaged using the Eclipse Ti microscope equipped with a DS-Fi1 camera (Nikon, Tokyo, Japan). The area where the invaded cells were occupied was quantified using the ImageJ software (NIH, Bethesda, MD).

2.7. Wound healing assay

A cell-based wound healing assay was performed according to the standard method. MDA-MB-231 cells were seeded by 2×10^5 cells/well in 6-well plates (Corning Inc., Corning, NY, USA) in 2 ml of DMEM supplemented with 10% FBS. Two days later, the cells reached 90% confluence and the monolayer was disrupted by a sterile pipette tip scraping the bottom of each well. Detached cells were washed out with PBS, and the remaining cells were cultured in serum-free DMEM containing different concentrations of PKI-402 (0, 0.02, 0.04 and 0.08 μM). 12 and 24 h post treatment, the wound edge closure towards which the cells migrated was monitored using Eclipse Ti microscope with DS-Fi1 camera (Nikon, Tokyo, Japan). The width of the wound edge closure was measured by Image-Pro Plus software (Media Cybernetics, Rockville, MD, USA).

2.8. Quantitative RT-PCR analysis

Bone tissue RNA was extracted from hind limb of the mice. Femur and tibia of the mice were ground using liquid nitrogen and RNA was isolated by Trizol reagent according to the manufacturer's instruction (Thermo Fisher Scientific, Waltham, MA, USA). The concentration of RNA was

determined by measuring the absorbance at 260 nm using NanoDrop TM ND-2000 spectrophotometer (Thermo Fisher Scientific, Waltham, MA, USA). For RT-PCR, cDNA was synthesized by reverse transcriptase with an oligo-dT primer. Expression levels of genes were assessed by RT-PCR, where cDNA was amplified by gene-specific primers and SYBR Green PCR MasterMix (ROCHE, Germany). Specific primers were used to quantify the following genes: *Cathepsin K* (Forward:5′-CTTCCAATACGTGCAGCAGA-3'; Reverse:5′-TCTTCAGGGCTTTCTCGTTC-3′), *CTR* (Forward:5′-TGCAGACA ACTCTTGGTTGG-3'; Reverse:5′-TCGGTTTCTTCTCCTCTGGA-3′), *NFATc1* (Forward:5′-CCGTTGCTTCCAGAAAATAAC-3'; Reverse:5′-TGTGGGATGT GAACTCGGA-3′), *V-ATPase-d2* (Forward:5'-AAGCCTTTGTTTGACGCTGT; Reverse:5′-TTCGATGCCTCTGTGAGATG-3′), *ACP5* (Forward:5′-CACTCCC ACCCTGAGATTTGT-3'; Reverse:5′-CCCCAGAGACATGATGAAGTCA-3′), *c-Fos* (Forward; 5'—CCAGTCAAGAGCATCAGCAA-3; Rverse; 5′-AAGTAG TGCAGCCCGGAGTA-3′), *DC-STAMP* (Forward:5′-AAACCCTTGGGCTGTT CTT-3'; Reverse:5′-AATCATGGACGACTCCTTGG-3′), *β-actin* (Forward: 5′-TCTGCTGGAAGGTGGACAGT-3'; Reverse:5′-CCTCTATGCCAACACAG TGC-3′), *BAX* (Forward:5′-GCCCTTTTGCTTCAGGGTTT-3'; Reverse: 5′-CATCCTCTGCAGCTCCATGT-3′), *BCL2* (Forward:5′-GAACTGGGGGAG GATTGTGG-3'; Reverse:5′-CCGTACAGTTCCACAAAGGC-3′), *Caspase-3* (Forward:5′-CATGGAAGCGAATCAATGGACT-3'; Reverse:5′-CTGTACCAG ACCGAGATGTCA-3′), *Caspase-8* (Forward:5′-CTGGTCTGAAGGCTGGT TGT-3'; Reverse:5′-CAGGCTCAGGAACTTGAGGG-3′), *Caspase-9* (Forward: 5′-CAGGCCCCATATGATCGAGG-3'; Reverse:5′-TCGACAACTTTGCTGCT TGC-3′). The conditions are as follows: 95 °C for 10 min, followed by 35 cycles of 94 °C (40s), 60 °C (40s), 72 °C (40s), followed by an elongation step of 5 min at 72 °C. The target gene expression was normalized to the level of β-actin gene and all experiments were performed in triplicate.

2.9. Tumor xenografts

A mouse model of bone osteolysis was established to measure the *in vivo* osteolytic effect induced by breast cancer. Healthy female 6-week-old BALB/c nude mice purchased from Shanghai SLAC Laboratory Animal Co. Ltd (Shanghai, China) were randomly divided into 3 groups:sham group (n = 6), vehicle group (injection with MDA-MB-231 cells alone, n = 6) and PKI-402 group (injection with MDA-MB-231 cells and PKI-402, n = 6). After anesthetized with 3.5% chloral hydrate through peritoneal injection, 50 μl of MDA-MB-231 cells suspension (1×10^7 cells/ml) was injected into the proximal chamber of left tibia through the tibia plateau. Abdominal administration of PKI-402 (25 mg/kg) was performed every other day for 4 weeks after injection of the cells in PKI-402 group while the sham group and the vehicle group received PBS only. After 4 weeks, the tumor volume was measured using the following equation ($V = 0.2618 \times L \times W \times (L + W)$, W: the average distance in the proximal tibia at the level of the knee joint in the anterior-posterior and medial-lateral planes; L: the distance from the edge of the proximal of the tumor to the distal extent of tumor [12]). After euthanization, the right hind limb of each mouse was harvested for the measurement of osteoclast related gene expression, and the left tibia was fixed with 4% paraformaldehyde for micro-CT scanning and histological analysis.

2.10. Micro-CT scanning

After fixation, the right tibia was imaged by high resolution micro-CT scanner (Skyscan 1766, Bruker, Belgium). The growth plate was regarded as a reference. For trabecular bone, 100 slices were selected which begins from 50 slices away from the reference for analysis. For cortical bone, 100 slices were selected which begins from 400 slices away from the reference for analysis. Several trabecular and cortical bone parameters were measured including bone volume per tissue volume (BV/TV), bone surface per tissue volume (BS/TV), trabecular thickness (Tb. Th), trabecular number (Tb. N), Cortical crossectional Area (Ct. Ar) and Cortical Thickness (Ct. Th). Representative tibia 3D reconstruction was made by CTvox software.

2.11. H&E staining

After micro-CT scanning, the left hind limb and tumor tissue of each animal were decalcified in 10% EDTA for 4 weeks and paraffin-embedded. Serial sections were cut and mounted onto coated slides. The sections were deparaffinised by xylene, and treated with gradual concentrations of ethanol to deionized water. The sections were stained with eosin and haematoxylin and imaged under an optical microscope (Leica, Germany).

2.12. Immunohistochemical staining

Fixed and decalcified tibias were embedded in paraffin for tissue section. After dewaxing in xylene and rehydration in a gradient of ethanol concentrations, sections were incubated with anti-Cathepsin K and Caspase-3 antibody at 4 °C overnight. Then, the sections were incubated with an IgG-HRP polymer and diaminobenzidine substrate at 37 °C for 10–30 min. Sections were imaged under an optical microscope (Leica, Germany).

2.13. Western blot assays

Nearly confluence BMMs cultured in 6-well plates were serum starved for 4 h followed by the stimulation of 50 ng/mL RANKL for 0, 5, 10, 20, 30 and 60 min with or without PKI-402. Cellular protein was extracted by lysing cells using RIPA solution supplemented with protease and phosphatase inhibitors (Roche Diagnostics, Indianapolis, IN, USA). The protein was subjected to SDS-PAGE and transferred to the nitrocellulose membrane (Millipore, Billerica, MA, USA). After blocking with 5% BSA, the membrane was incubated at 4 °C overnight with primary antibodies which were diluted according to the manufacturer's instruction. After washed with 1 × TBST, the membrane was incubated with second antibody for 1 h at room temperature. The immunoreactivity was detected by Odyssey V3.0 image scanner (Li-COR, Lincoln, NE, USA). ImageJ software was used to analyze strip strength.

2.14. Alkaline phosphatase staining

Osteoblasts were isolated from the calvariae of newborn SD rats. Cells were seeded onto a 24-well plate by 5×10^4 cells/well and cultured in differentiation medium (DMEM containing 10% FBS, 50 μg/ml ascorbic acid, 5 mM β-glycerophosphate and 10^{-8} M dexamethasone) with different concentrations of PKI-402 for 7 days. The cell culture medium was changed every 3 days. Then the cells were fixed using 4% paraformaldehyde and stained with Alkaline phosphatase (ALP) BCIP/NBT Liquid Substrate System Kit (Sigma Aldrich) for 10 min. The result of staining is observed under an optical microscope (Leica, Germany).

2.15. Statistical analysis

The numerical value was expressed as average ± standard deviation (SD) for the three or more experiments. SPSS v.13.0 software (IBM, Armonk, NY, USA) was used to analyze the results. The differences between groups were evaluated by student's *t*-test. Differences with P values of < 0.05 were considered statistically significant.

3. Result

3.1. PKI-402 inhibits RANKL-induced osteoclastogenesis

To study the effect of PKI-402 (chemical structure shown in Fig. 1A) on osteolysis induced by breast cancer, we initially assessed its effect on the cell proliferation of bone marrow derived monocytes/macrophages (BMMs) using the MTS assay. The results showed that the cell growth was not affected by 0.08 μM of PKI-402 until 72 h (Fig. 1B). RANKL-induced osteoclastogenesis was observed as TRAP-positive cells that

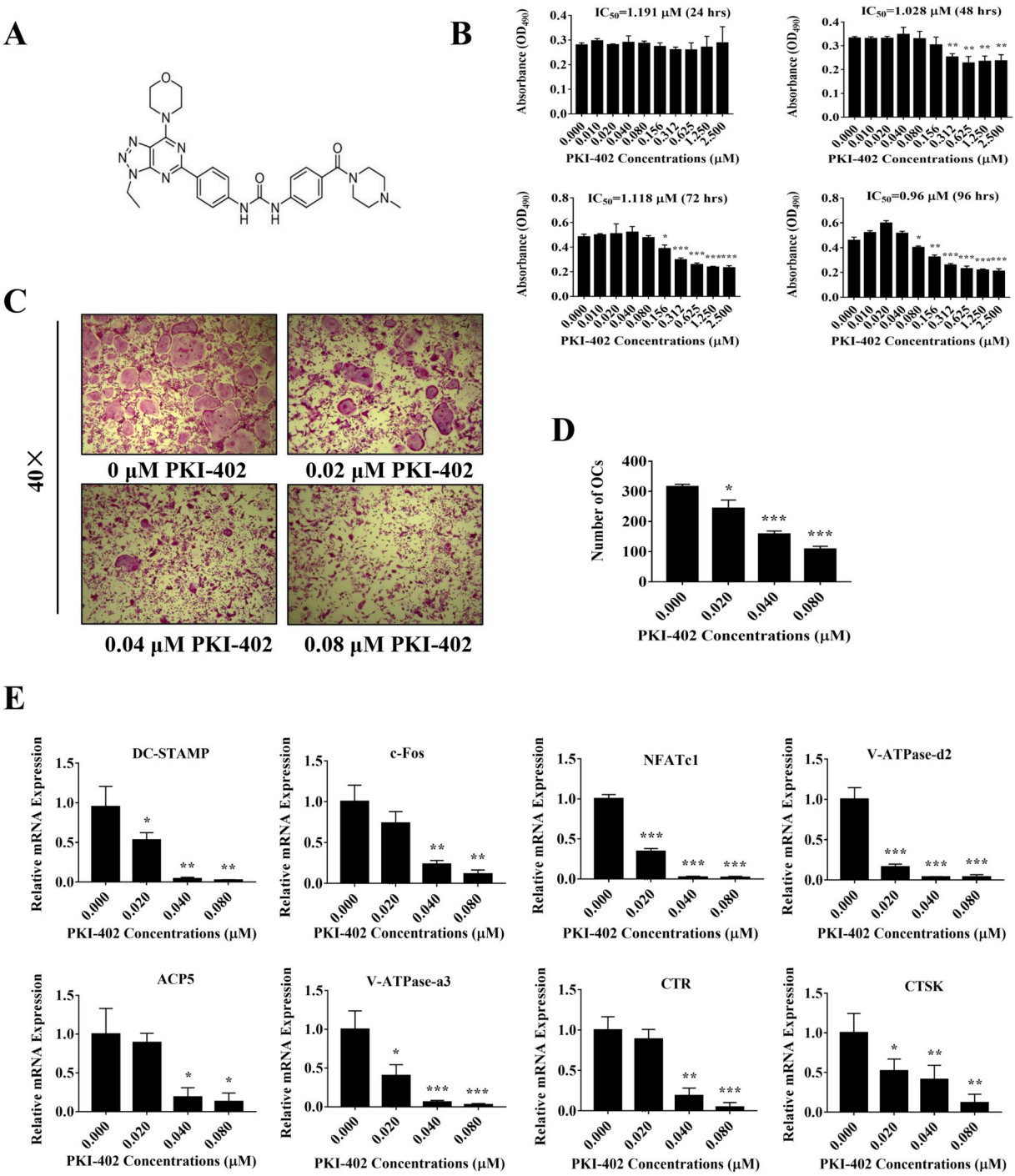

Fig. 1. PKI-402 inhibits RANKL-induced osteoclastogenesis andosteoclast-specific gene expression. (A) The chemical structure of PKI-402. (B) Decreased proliferation of mouse bone marrow-derived macrophages (BMMs) by PKI-402. BMMs were treated with the indicated concentration of PKI-402. Cell proliferation was measured using MTS assay. The calculated IC50 for PKI-402 in BMMs at 24, 48, 72 and 96 h were shown. (C) TRAP staining of BMMs that were treated with the indicated concentrations of PKI-402, 30 ng/ml M-CSF and 50 ng/ml RANKL for 5 days. (D) Quantitation of the numbers of osteoclasts (OCs) identified as TRAP-positive cells. (E) Decreased expression levels of osteoclast-specific genes by PKI-402. BMMs were cultured with the indicated concentrations of PKI-402, 30 ng/ml M-CSF, and 50 ng/ml RANKL until mature osteoclasts were observed. Expression of osteoclast-specific genes was measured by real-time PCR. All experiments are replicated 3 times. Data are presented as mean ± SD; *p < 0.05, **p < 0.01, ***p < 0.001 relative to RANKL alone-induced controls.

were found when the cells were incubated with M-CSF and RANKL for 5 days. By contrast, PKI-402 treatment led to significant decreases in the number of multinucleated osteoclast-like cells in a concentration-dependent manner (Fig. 1C and D). Consistent with the observation, expression levels of osteoclast-related genes, such as *DC-STAMP*, *c-Fos*, *NFATc1*, *V-ATPase-d2*, *V-ATPase-a3, ACP5*, *CTR*, and *Cathepsin K* (*CTSK*), were reduced significantly when treated with PKI-402. For example, gene expression levels of *DC-STAMP*, *c-Fos* and *CTSK* were decreased by 97%, 88%, and 87%, respectively (Fig. 1E). Taken together, these data strongly suggested that PKI-402 inhibited

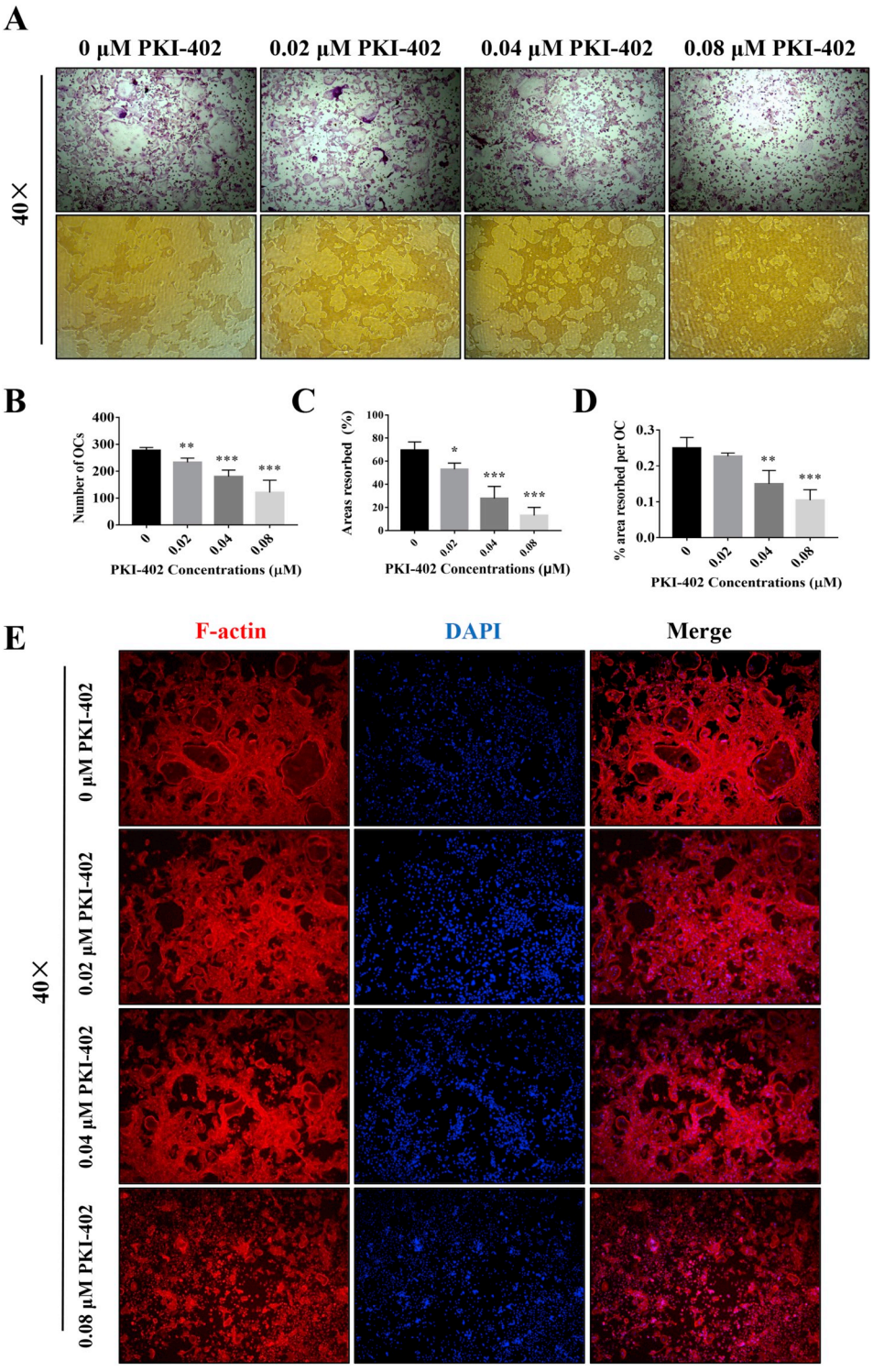

Fig. 2. PKI-402 inhibits RANKL-induced hydroxyapatite resorption and the formation of F-actin ring. (A) Representative images of TRAP staining and hydroxyapatite resorption and (B) Quantitation of the numbers of osteoclasts (OCs) identified as TRAP-positive cells, (C) the percentage of the area of hydroxyapatite resorption and (D) the percentage of the area of hydroxyapatite resorption per osteoclast. (E) Representative images of osteoclasts stained for F-actin rings (phalloidin) and nuclei (DAPI). All experiments are replicated 3 times. Data are presented as mean ± SD; *p < 0.05, **p < 0.01, ***p < 0.001 relative to RANKL alone-induced controls.

osteoclastogenesis *in vitro*, namely RANKL-induced differentiation of monocyte to osteoclasts.

3.2. PKI-402 inhibits osteoclastic bone resorption and the formation of F-actin ring

Osteoclastogenesis is multiple stages of the complicate process, including commitment, differentiation, multinucleation and activation of immature osteoclasts [13]. To investigate whether PKI-402 affected bone resorption mediated by mature osteoclasts, pre-mature osteoclasts were seeded onto the hydroxyapatite plate and cultured for 48 h with or without PKI-402. We observed a 69.5% of hydroxyapatite was resorbed in the control group. However, treatment with PKI-402 at 0.08 μM caused about 15.0% reduction in resorption area. The analysis showed that the percentage of the hydroxyapatite resorption area of mature osteoclasts was greatly decreased at 0.02 or 0.04 μM and the nearly inhibition when cells treated with 0.08 μM of PKI-402 (Fig. 2A–C). Since the formation of osteoclasts was also inhibited at 0.08 μM of PKI-402 (Fig. 2A and B), we further investigated the absorption area of each osteoclast in the presence of PKI-402. We found that PKI-402 still

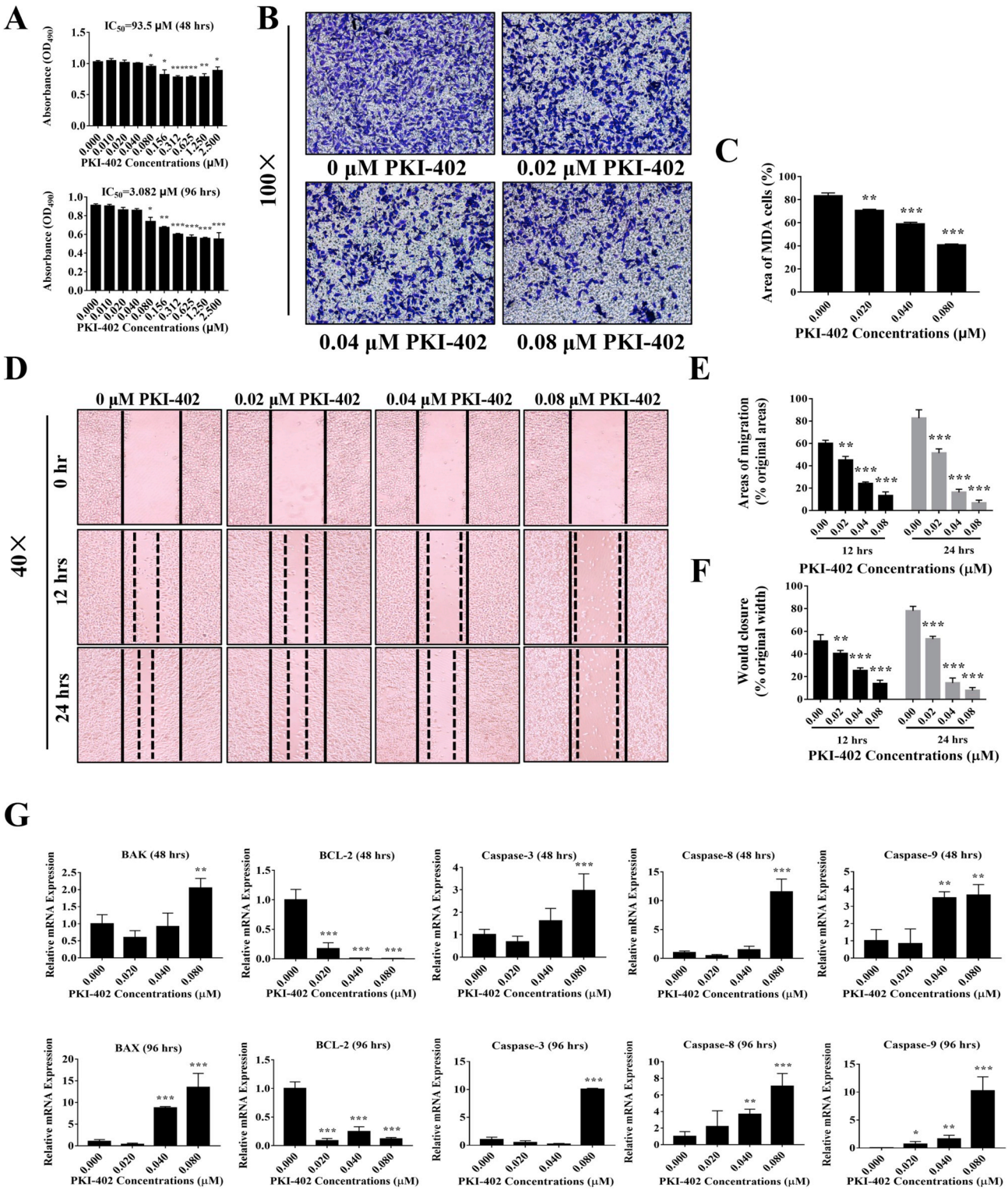

Fig. 3. PKI-402 inhibits the proliferation, invasion and migration of MDA-MB-231 cells. (A) Decreased proliferation of MDA-MB-231 cells by PKI-402. The calculated IC50 for 48 and 96 h was shown. (B) Reduced invasion of MDA-MB-231 cells by PKI-402. MDA-MB-231 breast cancer cells treated with the indicated concentrations of PKI-402 for 24 h in the Transwell assay were stained with crystal violet. (C) Quantitation of the areas of invasive cells. (D) Reduced migration of MDA-MB-231 cells by PKI-402. Solid lines indicate the borders of the wound edge closure at 0 h. Dash lines indicate the borders of the migrating cells reached at 12 and 24 h. (E and F) Quantitation of the areas of migrating cells and the width of the wound edge closure by migrating cells using ImageJ software. (G) Real-time PCR analysis of the expression levels of apoptosis-associated genes in MDA-MB-231 cells treated with the indicated concentrations of PKI-402 for 48 or 96 h. All experiments are replicated 3 times. Data are presented as mean ± SD; *$p < 0.05$, **$p < 0.01$, ***$p < 0.001$ relative to RANKL alone-induced controls. (For interpretation of the references to colour in this figure legend, the reader is referred to the Web version of this article.)

inhibited the area of absorption by each osteoclast at concentrations of 0.04 μM and 0.08 μM (Fig. 2D). The fusion of osteoclasts and the formation of F-actin after PKI-402 treatment were significantly reduced, especially at 0.08 μM (Fig. 2E). These results demonstrated that PKI-402 inhibited bone resorption of osteoclasts and the formation of F-actin ring.

3.3. PKI-402 inhibits the proliferation, migration and invasion of MDA-MB-231 breast cancer cells in vitro

We next examined whether treatment of PKI-402 might affect proliferation of MDA-MB-231 breast cancer cell line like BMMs. The results of the MTS cell proliferation assay showed that the calculated IC_{50} values of PKI-402 at 48 and 96 h were 93.5 and 3.1 μM, respectively (Fig. 3A). PKI-402 also blocked invasion (Fig. 3B and C) and migration (Fig. 3D–F) of MDA-MB-231 cells in a concentration-dependent manner. Furthermore, the treatment of PKI-402 led to down-regulation of the anti-apoptotic gene *BCL-2* and up-regulation of the apoptotic genes, including *BAX*, *Caspase-3*, *Caspase-8* and *Caspase-9* in MDA-MB-231 cells (Fig. 3G). Taken together, these results demonstrated that PKI-402 suppresses proliferation, invasion and migration of breast cancer cells *in vitro*.

3.4. PKI-402 inhibits breast cancer induced osteolysis

Given the inhibitory effects of PKI-402 on formation of osteoclasts, bone resorption of mature osteoclasts, and proliferation, invasion and migration of breast cancer cells, we investigated the *in vivo* effect of PKI-402 on breast cancer-induced osteolysis. MDA-MB-231 breast cancer cells were injected into the tibia compartment of BALB/c nude mice, followed by administration of PKI-402 to animals every other day for 28 days. We found that PKI-402 reduced the tumor growth (Fig. 4A and B) and analysis of micro-CT scanning technique clearly showed that PKI-402 blocked breast cancer-induced bone destruction (Fig. 4C). The quantitation results showed that while the bone volume and bone surface were decreased upon the injection of breast cancer cells, administration of PKI-402 led to both parameters returning to the levels as the control group. However, there is no significant effect on trabecular thickness (Tb. Th) and trabecular separation (Tb. Sp) among 3 groups (Fig. 4D, Fig. S1A). Consistent with analysis of micro-CT images, the presence of tumor cells in the PKI-402 group was greatly reduced (Fig. 4E). The results of immunohistochemistry showed that the expression of Cathepsin K was reduced after PKI-402 treatment, and PKI-402 could promote the expression of the apoptotic protein Caspase-3 (Fig. 4F). The expression levels of osteoclast-related genes *in vivo* including *DC-STAMP, NFATc1, V-ATPase-d2, c-Fos, CTR, and, CTSK were inhibited by PKI-402* (Fig. 4G). Taken together, PKI-402 suppressed tumor growth, and blocked breast cancer induced-bone destruction *in vivo*.

3.5. PKI-402 inhibits breast cancer-induced osteoclast differentiation by impairing the PI3K-AKT-mTOR signaling pathways

To determine whether PKI-402 could indeed inhibit the PI3K/AKT/mTOR signaling pathway in BMMs under RANKL stimulation, we examined protein expression levels in the cells treated with PKI-402 by western blotting. BMMs were pretreated with 0.08 μM PKI-402 for 1 h followed by stimulation of RANKL for 0, 5, 10, 20, 30, and 60 min. The level of phosphorylated m-TOR was increased upon RANKL stimulation at 20 min. However, this activation was suppressed by PKI-402 (Fig. 5A). Similarly, PKI-402 also greatly reduced the levels of activated p-P85, and *p*-AKT while the total protein levels of mTOR, P85 and AKT were not affected (Fig. 5A). Similarly, the levels of phosphorylated AKT and mTOR in MDA-MB-231 cells were also similarly reduced by PKI-402 (Fig. 5B). These results indicated that PKI-402 inhibited PI3K-AKT-mTOR pathway in both BMMs and MDA-MB-231 cells.

4. Discussion

The complications caused by bone metastasis in breast cancer seriously affect patients' quality of life [14]. Active osteoclast bone resorption play critical roles in tumor associated bone destruction [15]. Osteoclast can be activated by breast cancer which express RANKL [16]; Osteoclasts can release growth factor such as TGF-beta, IGF, IL-6 and IL-11 to promote breast cancer proliferation [17].

In this study, we demonstrated that treatment of PKI-402 leads to inhibition of differentiation and functions of osteoclasts, as evidenced by suppression of osteoclast formation, decreased expression of osteoclastic-specific genes and inhibition of osteoclast-mediated bone resorption. The inhibition of actin ring formation and bone resorption may be likely to be due to inhibition of osteoclast formation rather than inhibition of the activity of mature, healthy osteoclasts. So further research will be continued in the future. PKI-402 also reduces the abilities of MDA-MB-231 breast cancer cells to proliferate, migrate and invade the extracellular matrix. It is well established that ER + cells metastasizes to bone at much higher frequency than triple negative breast cancer cells [18]. Since MDA-231 cells have been shown to metastasize to bone and cause osteolysis [19–21], in this study, we confirmed PKI-402 inhibited MDA-MB-231-induced osteolysis *in vivo*, and selected MDA-231 cells for animal model in this experiment. However, the effect of PKI-402 on other cell lines of breast cancer was not evaluated. The effect of PKI-402 on other cell lines of breast cancer will be explored in future experiments.

In *in vivo* study, the whole volume of the tumor (within and out of the bone) were measured which represented the clinical setting more closely. Tumor volume measurements (volume = (L + W) (L) (W) (0.2618)), W: the average distance in the proximal tibia at the level of the knee joint in the anterior-posterior and medial-lateral planes; L: the distance from the edge of the proximal of the tumor to the distal extent of tumor) are based on references [12]. Micro CT analysis is a general tool for bone volume measurement, and the specific micro CT analysis procedure was as described in methods. There seems to be an upward trend in Tb.Sp, but later analysis shows no statistical difference. 3D images of the trabecular bone only were reconstructed, which showed that cancellous bone is increased after PKI-402 treatment (Fig. S1A).

Both analyses of micro-CT images and histology showed that the administration of PKI-402 *in vivo* greatly reverses bone damage caused by breast cancer. PKI-402 had no apparent effect on osteoblast differentiation at the concentration which inhibits osteoclast formation (Fig. S2A). We also found that PKI-402 has no significant effect on cortical bone *in vivo*, which is consistent with *in vitro* result (Fig. S2B-C). These results strongly suggest that targeting the signaling pathway involved in formation and functions of osteoclasts may be a good therapeutic option for breast cancer-associated osteolysis.

PI3K/mTOR signaling pathway is an important target for breast cancer [22]. In human sample, the PI3K/mTOR protein is highly expressed in many human tumors, such as breast cancer, prostate cancer, lung cancer and liver cancer [23,24]; It is reported in nude mice experiment, the PI3K/mTOR protein is expressed and increased after tumor formation in mice [25]. The abnormality of PI3K/mTOR signal transduction pathway is an important step in the development and progression of cancer since it plays an important role in tumor cell proliferation, survival, resistance to apoptosis, angiogenesis and metastasis, and resistance to radiochemotherapy [26,27]. Currently, A variety of inhibitors with PI3K/mTOR pathway as the target have become the research hotspot [28,29]. Many drugs targeting molecules in this pathway are being studied in preclinical or clinical trials [30,31]. In this study, we used the newly synthesized compound PKI-402 and confirmed its inhibitory effects on breast cancer cell proliferation, apoptosis and migration *in vivo*. This finding is in line with Robert Mallon [10]. However, they have not yet explored whether PKI-402 can inhibit breast cancer induced osteolysis. Therefore, we take a further step to investigate this effect and found that PKI-402 can also prevent

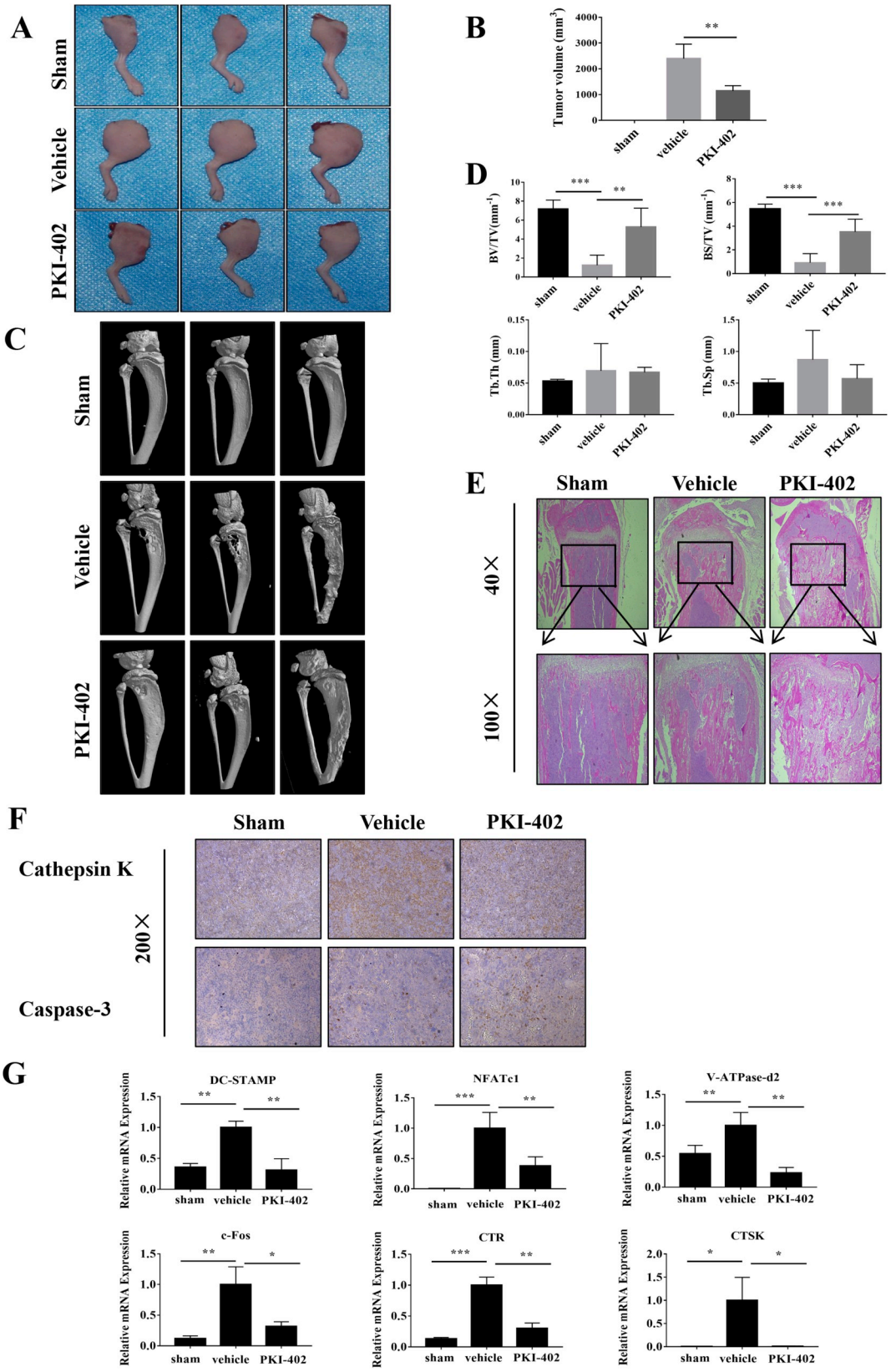

Fig. 4. PKI-402 inhibits tumor growth and breast cancer-associated osteolysis *in vivo*. (A) Representative images of the hind limb of mice where MDA-MB-231 cells were injected into the tibial marrow cavity. n = 6. (B) Quantitation of the tumor volume of mice in each group. (C) Representative micro-CT 3-dimensional reconstructed images for each group of mice. (D) Quantitation of bone volume per tissue volume (BV/TV), bone surface per tissue volume (BS/TV), trabecular thickness (Tb. Th) and trabecular number (Tb. N) in each group of mice. (E) Representative H&E images of the tibia in each group of mice. (F) Representative Immunohistochemical staining images in each group of mice. (G) Real-time PCR analysis of the expression levels of osteoclast-related genes in each group of mice. The experiment was replicated 3 times. Data are presented as mean ± SD; *p < 0.05, **p < 0.01, ***p < 0.001 relative to RANKL alone-induced controls.

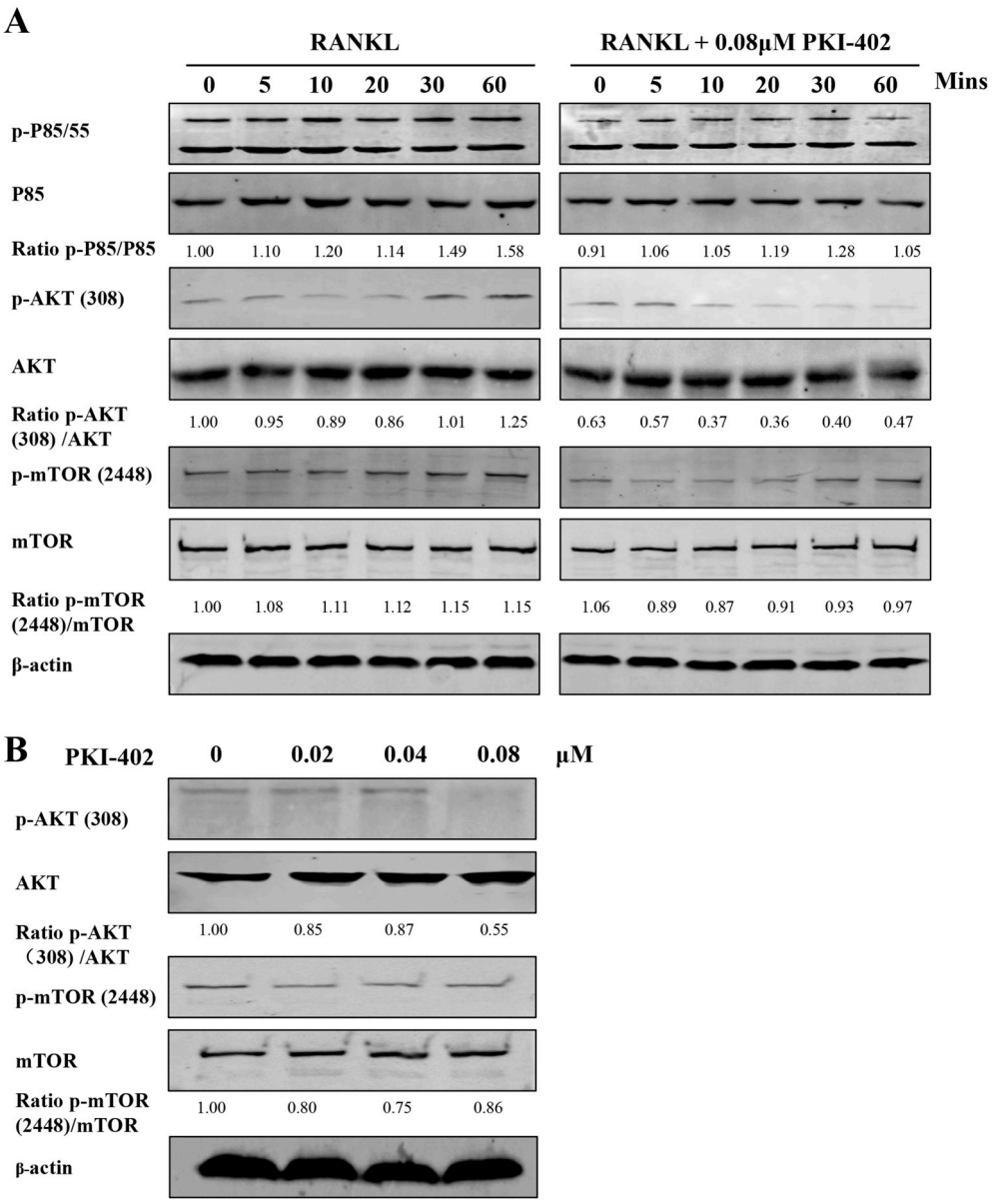

Fig. 5. PKI-402 inhibits breast cancer-induced osteoclast differentiation by suppressing the PI3K-AKT-mTOR pathway. (A) BMMs were pre-treated with or without PKI-402 at 0.08 μM for 1 h followed by stimulation of 50 ng/ml RANKL for the indicated time (0, 5, 10, 20, 30, or 60 min). (B) MDA-MB-231 cells were treated with indicated concentration of PKI-402 for 1 h. Cell lysates were analyzed using western blotting for proteins in the PI3K/AKT/mTOR signaling pathway. The ratio of the density of bands shown below was determined using Image J.

breast cancer induced bone destruction via suppression PI3K-AKT-mTOR signaling pathway both in BMMs and breast cancer cells. Everolimus (an mTOR inhibitor) has been approved for the treatment of metastatic ER + breast cancer [32]. However, everolimus has a series of side effects such as stomatitis, noninfectious pneumonitis, infections, rash et al. [33]. In this study, we didn't compare the effect of PKI-402 and everolimus for the treatment of metastatic ER + breast cancer. Further explore on the effects of PKI-402 for the treatment of metastatic ER + breast cancer in future research is needed.

Regarding the animal model, we injected tumor cells directly into the medullary cavity instead of injecting the heart. Although this limitation does not well mimic the distant metastasis of tumor cells, it is directly responsible for bone destruction. In addition, we did not evaluate the toxic side effects of PKI-402 in detail. This will be carefully studied in the next research.

In summary, this study demonstrated the novel PI3K-mTOR inhibitor PKI-402 is effective in preventing breast cancer induced osteolysis via inhibiting both osteoclast function and breast cancer cell function. Therefore, this compound is potential for further pre-clinical evaluation for the treatment of breast cancer induced osteolysis.

Conflicts of interest

The authors declare no conflict of interest.

Acknowledgement

This project is supported in part by National Natural Science Foundation of China (81501910), the Natural Science Foundation of Guangdong Provinve (2018A030307025), the Natural Science Foundation of Guangxi Province (2015GXNSFCA414001, 2015GXNSFDA139019) and Guangxi science and technology project (Guikehe1599005-2-12).

Appendix A. Supplementary data

Supplementary data to this article can be found online at https://doi.org/10.1016/j.canlet.2018.11.038.

References

[1] L. Fan, K. Strasser-Weippl, J.-J. Li, J. St Louis, D.M. Finkelstein, K.-D. Yu, W.-Q. Chen, Z.-M. Shao, P.E. Goss, Breast cancer in China, Lancet Oncol. 15 (2014) e279–e289.

[2] M. Croset, D. Goehrig, A. Frackowiak, E. Bonnelye, S. Ansieau, A. Puisieux, P. Clezardin, TWIST1 expression in breast cancer cells facilitates bone metastasis formation, J. Bone Miner. Res.: Off. J. Am. Soc. Bone and Min. Res. 29 (2014) 1886–1899.

[3] L. Ye, M.D. Mason, W.G. Jiang, Bone morphogenetic protein and bone metastasis, implication and therapeutic potential, Front. Biosci. 16 (2011) 865–897.

[4] T. Shimizu, A.W. Tolcher, K.P. Papadopoulos, M. Beeram, D.W. Rasco, L.S. Smith, S. Gunn, L. Smetzer, T.A. Mays, B. Kaiser, M.J. Wick, C. Alvarez, A. Cavazos, G.L. Mangold, A. Patnaik, The clinical effect of the dual-targeting strategy involving PI3K/AKT/mTOR and RAS/MEK/ERK pathways in patients with advanced cancer, Clin. Canc. Res.: Off. J. Am. Assoc. Cancer Res. 18 (2012) 2316–2325.

[5] K.-K. Wong, J.A. Engelman, L.C. Cantley, Targeting the PI3K signaling pathway in cancer, Curr. Opin. Genet. Dev. 20 (2010) 87–90.

[6] L.F. Hernandez-Aya, A.M. Gonzalez-Angulo, Targeting the phosphatidylinositol 3-kinase signaling pathway in breast cancer, Oncology 16 (2011) 404–414.

[7] J.-Y. Shin, J.-O. Kim, S.K. Lee, H.-S. Chae, J.-H. Kang, LY294002 may overcome 5-FU resistance via down-regulation of activated p-AKT in Epstein-Barr virus-positive gastric cancer cells, BMC Canc. 10 (2010) 425.

[8] S.-M. Maira, S. Pecchi, A. Huang, M. Burger, M. Knapp, D. Sterker, C. Schnell, D. Guthy, T. Nagel, M. Wiesmann, S. Brachmann, C. Fritsch, M. Dorsch, P. Chene, K. Shoemaker, A. De Pover, D. Menezes, G. Martiny-Baron, D. Fabbro, C.J. Wilson, R. Schlegel, F. Hofmann, C. Garcia-Echeverria, W.R. Sellers, C.F. Voliva, Identification and characterization of NVP-BKM120, an orally available pan-class I PI3-kinase inhibitor, Mol. Canc. Therapeut. 11 (2012) 317–328.

[9] D.S. Hong, D.W. Bowles, G.S. Falchook, W.A. Messersmith, G.C. George, C.L. O'Bryant, A.C.H. Vo, K. Klucher, R.S. Herbst, S.G. Eckhardt, S. Peterson, D.F. Hausman, R. Kurzrock, A. Jimeno, A multicenter phase I trial of PX-866, an oral irreversible phosphatidylinositol 3-kinase inhibitor, in patients with advanced solid tumors, Clin. Canc. Res.: Off. J. Am. Assoc. Cancer Res. 18 (2012) 4173–4182.

[10] R. Mallon, I. Hollander, L. Feldberg, J. Lucas, V. Soloveva, A. Venkatesan, C. Dehnhardt, E. Delos Santos, Z. Chen, O. Dos Santos, S. Ayral-Kaloustian, J. Gibbons, Antitumor efficacy profile of PKI-402, a dual phosphatidylinositol 3-kinase/mammalian target of rapamycin inhibitor, Mol. Canc. Therapeut. 9 (2010) 976–984.

[11] C.M. Dehnhardt, A.M. Venkatesan, E. Delos Santos, Z. Chen, O. Santos, S. Ayral-Kaloustian, N. Brooijmans, R. Mallon, I. Hollander, L. Feldberg, J. Lucas, I. Chaudhary, K. Yu, J. Gibbons, R. Abraham, T.S. Mansour, Lead optimization of N-3-substituted 7-morpholinotriazolopyrimidines as dual phosphoinositide 3-kinase/mammalian target of rapamycin inhibitors: discovery of PKI-402, J. Med. Chem. 53 (2010) 798–810.

[12] H.H. Luu, Q. Kang, K.P. Jong, W. Si, Q. Luo, W. Jiang, H. Yin, A.G. Montag, M.A. Simon, T.D. Peabody, R.C. Haydon, C.W. Rinker-Schaeffer, T.C. He, An orthotopic model of human osteosarcoma growth and spontaneous pulmonary metastasis, Clin. Exp. Metastasis 22 (2005) 319–329.

[13] M.P. Yavropoulou, J.G. Yovos, Osteoclastogenesis–current knowledge and future perspectives, J. Musculoskelet. Neuronal Interact. 8 (2008) 204–216.

[14] D.H. Henry, L. Costa, F. Goldwasser, V. Hirsh, V. Hungria, J. Prausova, G.V. Scagliotti, H. Sleeboom, A. Spencer, S. Vadhan-Raj, R. von Moos, W. Willenbacher, P.J. Woll, J. Wang, Q. Jiang, S. Jun, R. Dansey, H. Yeh, Randomized, double-blind study of denosumab versus zoledronic acid in the treatment of bone metastases in patients with advanced cancer (excluding breast and prostate cancer) or multiple myeloma, J. Clin. Oncol.: Off. J. Am. Soc. Clin. Oncol. 29 (2011) 1125–1132.

[15] K.N. Weilbaecher, T.A. Guise, L.K. McCauley, Cancer to bone: a fatal attraction, Nat. Rev. Canc. 11 (2011) 411–425, https://doi.org/10.1038/nrc3055.

[16] V. Sigl, J.M. Penninger, RANKL/RANK - from bone physiology to breast cancer, Cytokine Growth Factor Rev. 25 (2014) 205–214.

[17] Y. Chen, D.M. Sosnoski, A.M. Mastro, Breast Cancer Metastasis to the Bone : Mechanisms of Bone Loss, (2010).

[18] W.D. Foulkes, I.E. Smith, J.S. Reis-Filho, Triple-negative breast cancer, N. Engl. J. Med. 363 (2010) 1938–1948.

[19] G. van der Pluijm, I. Que, B. Sijmons, J.T. Buijs, C.W.G.M. Lowik, A. Wetterwald, G.N. Thalmann, S.E. Papapoulos, M.G. Cecchini, Interference with the microenvironmental support impairs the de novo formation of bone metastases in vivo, Cancer Res. 65 (2005) 7682–7690.

[20] J.T. Buijs, N.V. Henriquez, P.G.M. van Overveld, G. van der Horst, I. Que, R. Schwaninger, C. Rentsch, P. Ten Dijke, A.-M. Cleton-Jansen, K. Driouch, R. Lidereau, R. Bachelier, S. Vukicevic, P. Clezardin, S.E. Papapoulos, M.G. Cecchini, C.W.G.M. Lowik, G. van der Pluijm, Bone morphogenetic protein 7 in the development and treatment of bone metastases from breast cancer, Cancer Res. 67 (2007) 8742–8751.

[21] J. Xu, S. Acharya, O. Sahin, Q. Zhang, Y. Saito, J. Yao, H. Wang, P. Li, L. Zhang, F.J. Lowery, W.-L. Kuo, Y. Xiao, J. Ensor, A.A. Sahin, X.H.-F. Zhang, M.-C. Hung, J.D. Zhang, D. Yu, 14-3-3zeta turns TGF-beta's function from tumor suppressor to metastasis promoter in breast cancer by contextual changes of Smad partners from p53 to Gli2, Cancer Cell 27 (2015) 177–192.

[22] K.D. Courtney, R.B. Corcoran, J.A. Engelman, The PI3K pathway as drug target in human cancer, J. Clin. Oncol.: Off. J. Am. Soc. Clin. Oncol. 28 (2010) 1075–1083.

[23] A.X. Zhu, T.A. Abrams, R. Miksad, L.S. Blaszkowsky, J.A. Meyerhardt, H. Zheng, A. Muzikansky, J.W. Clark, E.L. Kwak, D. Schrag, K.R. Jors, C.S. Fuchs, A.J. Iafrate, D.R. Borger, D.P. Ryan, Phase 1/2 study of everolimus in advanced hepatocellular carcinoma, Cancer 117 (2011) 5094–5102.

[24] J.A. Engelman, Targeting PI3K signalling in cancer: opportunities, challenges and limitations, Nat. Rev. Canc. 9 (2009) 550–562.

[25] J. Cebulla, E.M. Huuse, K. Pettersen, A. van der Veen, E. Kim, S. Andersen, W.S. Prestvik, A.M. Bofin, A.P. Pathak, G. Bjorkoy, T.F. Bathen, S.A. Moestue, MRI reveals the in vivo cellular and vascular response to BEZ235 in ovarian cancer xenografts with different PI3-kinase pathway activity, Br. J. Canc. 112 (2015) 504–513.

[26] H. Populo, J.M. Lopes, P. Soares, The mTOR signalling pathway in human cancer, Int. J. Mol. Sci. 13 (2012) 1886–1918.

[27] A. Arcaro, A.S. Guerreiro, The phosphoinositide 3-kinase pathway in human cancer: genetic alterations and therapeutic implications, Curr. Genom. 8 (2007) 271–306.

[28] S.K. Martin, S. Fitter, L.F. Bong, J.J. Drew, S. Gronthos, P.R. Shepherd, A.C.W. Zannettino, NVP-BEZ235, a dual pan class I PI3 kinase and mTOR inhibitor, promotes osteogenic differentiation in human mesenchymal stromal cells, J. Bone Miner. Res.: Off. J. Am. Soc. Bone and Mineral Res. 25 (2010) 2126–2137.

[29] B. Gobin, M.B. Huin, F. Lamoureux, B. Ory, C. Charrier, R. Lanel, S. Battaglia, F. Redini, F. Lezot, F. Blanchard, D. Heymann, BYL719, a new alpha-specific PI3K inhibitor: single administration and in combination with conventional chemotherapy for the treatment of osteosarcoma, Int. J. Canc. 136 (2015) 784–796.

[30] A. Akinleye, P. Avvaru, M. Furqan, Y. Song, D. Liu, Phosphatidylinositol 3-kinase (PI3K) inhibitors as cancer therapeutics, J. Hematol. Oncol. 6 (2013) 88.

[31] J. Abraham, PI3K/AKT/mTOR pathway inhibitors: the ideal combination partners for breast cancer therapies? Expert Rev. Anticancer Ther. 15 (2015) 51–68.

[32] T. Bachelot, C. Bourgier, C. Cropet, I. Ray-Coquard, J.-M. Ferrero, G. Freyer, S. Abadie-Lacourtoisie, J.-C. Eymard, M. Debled, D. Spaeth, E. Legouffe, D. Allouache, C. El Kouri, E. Pujade-Lauraine, Randomized phase II trial of everolimus in combination with tamoxifen in patients with hormone receptor-positive, human epidermal growth factor receptor 2-negative metastatic breast cancer with prior exposure to aromatase inhibitors: a GINECO study, J. Clin. Oncol.: Off. J. Am. Soc. Clin. Oncol. 30 (2012) 2718–2724.

[33] M. Aapro, F. Andre, K. Blackwell, E. Calvo, M. Jahanzeb, K. Papazisis, C. Porta, K. Pritchard, A. Ravaud, Adverse event management in patients with advanced cancer receiving oral everolimus: focus on breast cancer, Ann. Oncol.: Off. J. Europ. Soc. Med. Oncol. 25 (2014) 763–773.